Annual Progress Report 3, 2014-2015

NASA Award Number: NNX12AD28G

Global-scale assessment of threatened river delta systems: Evaluation of connections between the continental land mass and ocean through integrated remote sensing and process modeling.

City University of New York
Co-investigators: Charles J. Vörösmarty, Kyle McDonald, Balazs M. Fekete, Hansong Tang, Deborah Balk, Irina Gladkova, Michael Grossberg
Post-Doctoral Researcher: Zachary D. Tessler
PhD Students: Hannah Aizenman, Kat Jensen

University of Colorado
Co-I: James P.M. Syvitski
Research Scientist: Albert J. Kettner
Post-Doctoral Researcher: Stephanie Higgins
CSDMS, INSTAAR, Univ. of Colorado, 1560 30th St., Boulder CO, 80309
Award Number: PZ07124

1. Project overview

With population growth, development, and the specter of climate change-- sea level rise and changes in storm and flood surge exposure-- coastal wetland systems increasingly will become a major focal point of concern with respect to human vulnerability and sustainable development. The urgent need to study and develop a capacity to forecast the changing character of these linked geophysical-social systems serves as the chief impetus for our study. River deltas, in particular, are an important focal point for the impacts of humans on both terrestrial land mass and coastal zone systems, due to their position at the interface of these two major functional components of the Earth system. This project seeks to forward an integrated modeling and remote sensing system to assess their vulnerabilities by combining geophysical and social science perspectives. Our work is motivated by a major research challenge in the Earth system science: to identify, quantify, and understand how natural and human-dominated factors change freshwater discharge and riverborne sedimentary connections between the landmass and coastal ocean.

The overarching project **science goal** is "To analyze how the strength and variability of land-to-ocean links, as defined by riverine sediment fluxes, local anthropogenic activities and ocean processes, produce impacts on coastal delta systems, today and into the future."

Within this goal, during the 2014-2015 project year the University of Colorado worked on the following: 1) Mapping delta vulnerability based on changes in water and sediment flux and

ocean conditions, 2) Continued analysis of susceptible regions: The Ganges-Brahmaputra Delta, and 3) Methods of employing remote sensing for coastal ocean syndrome detection.

The CUNY team's efforts during this year have focused on 1) Retrospective landcover change analysis in case study deltas, 2) Improvement and downscaling of delta inundation mapping, 3) Synoptic-scale delta risk profiling and future vulnerability scenarios, 4) Empirical delta inundation modeling in case study deltas, and 5) Coastal ocean sediment modeling and sensitivity to delta river network structure.

Ongoing research efforts have been presented at several international conferences. Post-doctoral researcher Tessler co-convened a session at the AGU 2014 Fall Meeting entitled *"Impacts of Global Change on Deltas and Coastal Wetland Ecosystems: Scientific Advances in Support of Socioecological Resilience."* Team members also had a leadership presence at the "*Deltas in Times of Climate Change II*" International Conference in Rotterdam, The Netherlands, in September, 2014. Co-I Vörösmarty and Post-doc Tessler organized and chaired a workshop: "*Science-to-Action: Aligning science with stakeholder and community needs in the Mekong Delta system."*

Goals for the upcoming year focus on developing coastal delta population growth models and determination of changing risk patterns, extension of coastal modeling to additional case study deltas, and completion of delta wave energy analysis. Efforts this year will also be centered on preparing research results for publication, with several papers currently in preparation.

2. Research Progress 2014-2015

2.1. **Retrospective landcover change analysis (CUNY)**

The rapid growth of the populations and economies in populated delta regions has resulted in areas of large-scale land cover change. Development – agricultural, industrial, or urban – is known to displace flood-retention areas such as wetlands, forest, shrub, and bare lands. A preliminary study of the Mekong and Chao Phraya deltas was done to compare the patterns of land-use change that have occurred using historical Landsat imagery.

Three Landsat images, from similar seasons in each year, were selected from Landsat 5 TM [L5] and Landsat 7 ETM+ [L7] for each study area (Fig. 1) and processed through the USGS LEDAPS system. The atmospherically corrected bands 1-5 and 7, along with two indices – the widely used normalized difference vegetation index (NDVI) and the normalized difference water index (NDWI) – were used as inputs for supervised classification. Each image was classified into

five land cover classes: water (open water, flooded vegetation, aquaculture), sparse vegetation (shrub, grassland, senescing crops), dense vegetation (forest, peak healthy agriculture), built environment (concrete, asphalt, aluminum, etc), and bare land, using the maximum likelihood algorithm. Secondary data sources, such as aerial photographs, GoogleEarth and land cover maps from MODIS and GlobCover, were referred to when assigning training pixels for each land cover. More generalized classes are used because of the lack of detailed ground truth data. RGB composites of the Landsat imagery and the derived land cover classification maps are illustrated in Fig. 2 (Mekong) and Fig. 4 (Chao Phraya).

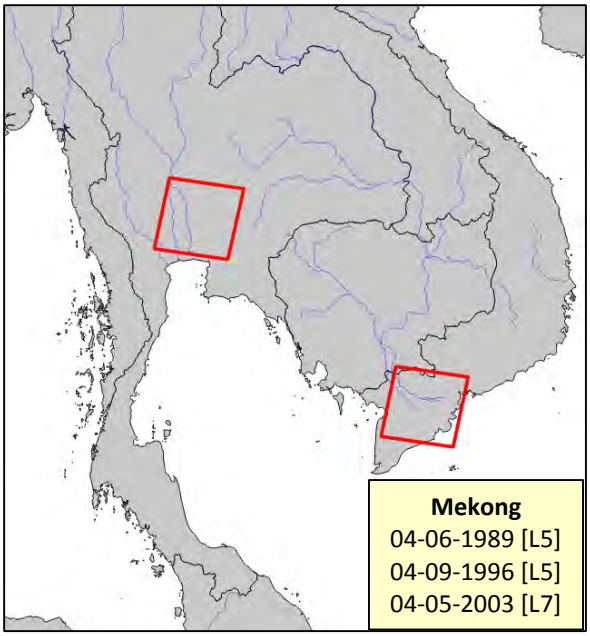

Fig. 1. Study areas: Mekong and Chao Phraya deltas. Image acquisition dates listed.

The proportion of each land cover type is shown Fig. 3 and Fig. 5 (Mekong and Chao Phraya, respectively), along with the change in area over time summarized in Table 1 and Table 2. The Mekong delta observed a decrease in bare area, increase in built environment and slight growth in overall vegetation. Agricultural areas were expanded in areas initially occupied by bare area by the building of embankments, dikes, and sluice gates in the late 1990s, according to census reports. Expansion of waterbodies can be potentially attributed to aquaculture ponds for fish and shrimp production. The built environment represents a much larger proportion of the scene over the Chao Phraya delta – which also observed substantial urban expansion from 1994 to 2004.

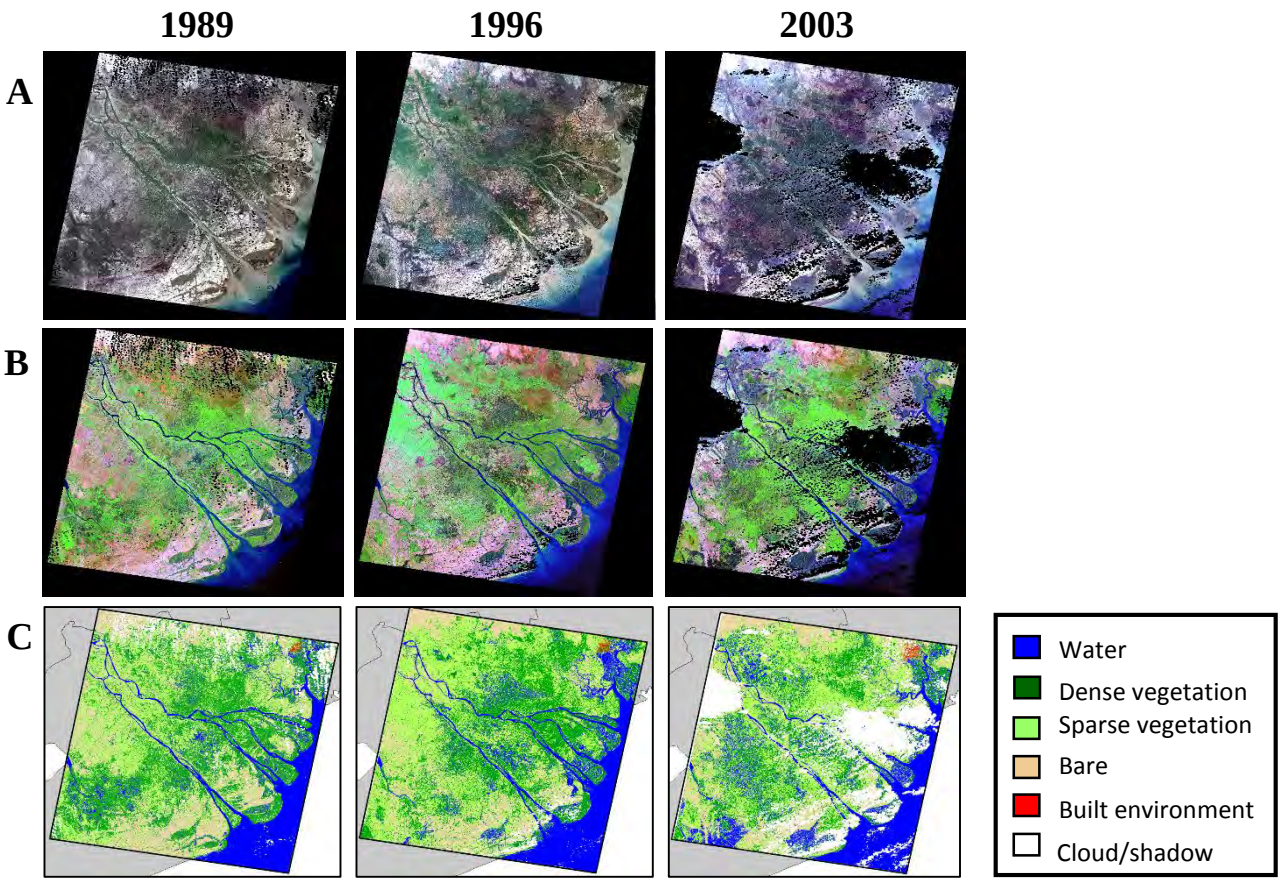

Fig. 2. Mekong delta Landsat imagery (A) "true color" composite RGB channels 3,2,1 (B) false-color composite RGB channels 5,4,2 (C) classified image results , from 1989, 1996, and 2003.

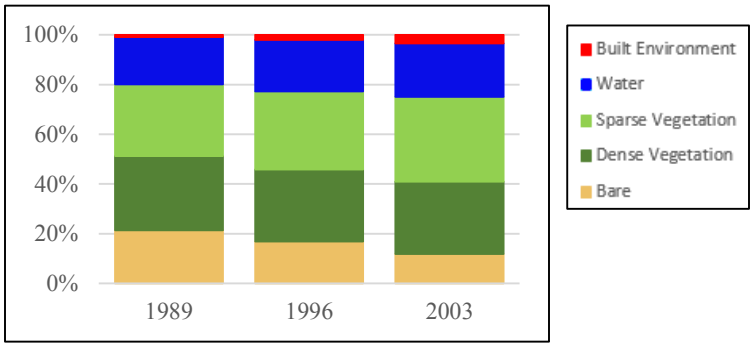

Fig. 3. Proportion of land cover in Mekong delta in 1989, 1996, and 2003, accounting only for pixels of which all three images have valid data).

Land Cover Class	Area (km^2) 1989	Area (km^2) 1996	% Change [since 1989]	Area (km^2) 2003	% Change [since 1989]
Built Environment	248	522	+110%	902	+264%
Water	5052	5538	+10%	5736	+14%
Sparse Vegetation	7697	8343	+8%	9048	+18%
Dense Vegetation	7980	7690	-4%	7725	-3%
Bare	5678	4462	-21%	3144	-45%

Table 1. Summary of land cover area and change, from 1989, 1996, and 2003. Only accounting for pixels that all three images have valid data.

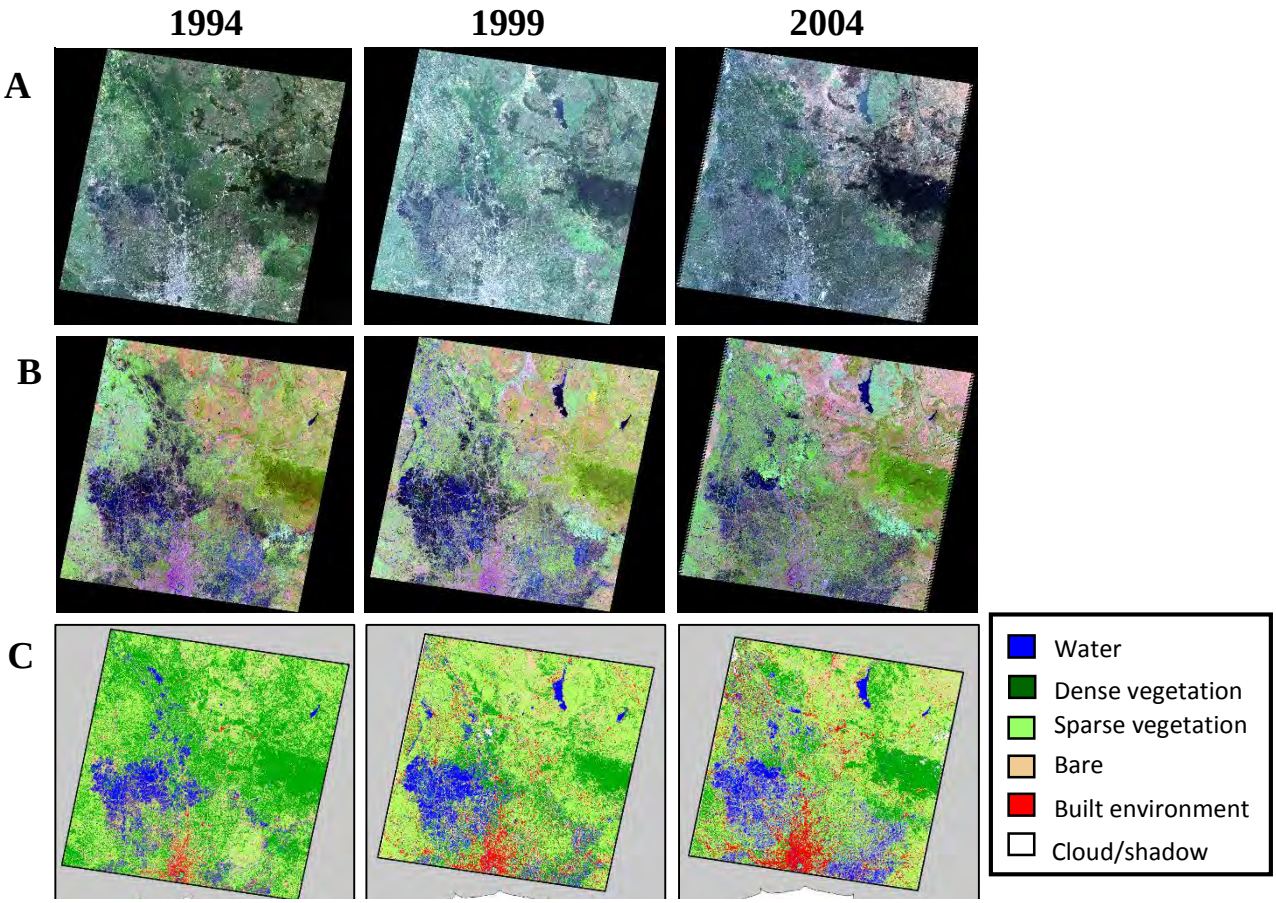

Fig. 4. Chao Phraya delta Landsat imagery (A) "true color" composite RGB channels 3,2,1 (B) false-color composite RGB channels 5,4,2 (C) classified image results , from 1994, 1999, and 2004.

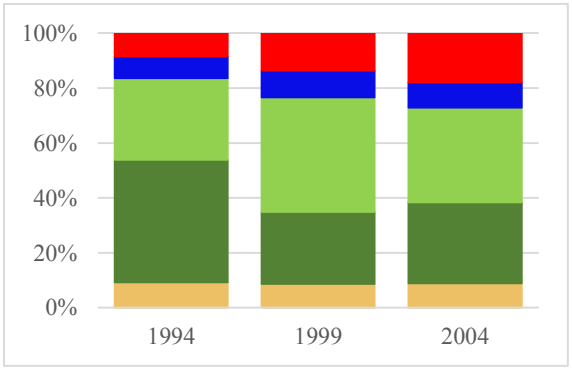

Fig. 5. Proportion of land cover in Chao Phraya delta in 1994, 1999, and 2004, accounting only for pixels of which all three images have valid data).

Land Cover Class	Area (km^2) 1994	Area (km^2) 1999	% Change [since 1994]	Area (km^2) 2004	% Change [since 1994]
Built Environment	2599	4188	+61%	5534	+113%
Water	2474	3011	+22%	2849	+15%
Sparse Vegetation	9152	12892	+40%	10647	+16%
Dense Vegetation	13787	8119	-41%	9100	-34%
Bare	2857	2659	-7%	2739	-4%

Table 2. Summary of land cover area and change, from 1994, 1999, and 2004. Only accounting for pixels that all three images have valid data.

2.2. **Improvement and Downscaling of Delta Inundation Mapping (CUNY)**

The Surface Water Microwave Product Series (SWAMPS) is a global time series of inundated area fraction (f_w) that is derived from passive and active microwave data (SSM/I, ERS, QuikSCAT, ASCAT) developed as part of a NASA MEaSUREs project. The most recent version of this product extends from 1992 to 2013, allowing large-scale assessment of hydrological baselines, dynamics, and trends at 25km resolution. We are interested in applying a physical downscaling algorithm to reduce the spatial resolution to ~100m. (Fig. 6) Topography from the Shuttle Radar Topography Mission (SRTM) digital elevation model, stream networks from Hydrosheds, and a permanent water cover mask derived from Landsat will be combined compute a static, relative "floodability" ranking representing the likelihood of flooding at each grid point relative to those in the surrounding area. We are currently working on developing this framework.

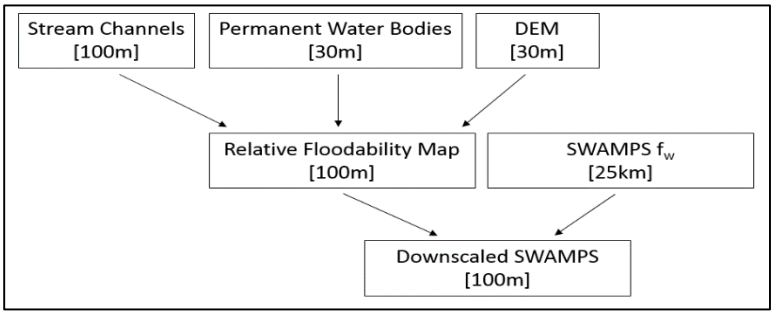

Fig. 6. Flow chart of SWAMPS downscaling process.

With the recent launch of NASA's Soil Moisture Active Passive (SMAP) that offers 1-3km spatial resolution L-band radar data with 3-day global coverage, we will be capable of generating higher resolution, operational surface water maps with frequent revisit intervals. We aim to produce and assess three variants of a SMAP-derived surface water dataset: (a) 1-km open-water map derived from a radiometric thresholding scheme produced approximately weekly, (b) 1-km weekly inundation fraction derived from a semi-empirical retrieval algorithm, and (c) 3-km inundation fraction produced in a similar fashion as (b) but with lower spatial resolution but greater temporal fidelity (~3-day). The SWAMPS dataset will be extended to the present time to perform a product comparison with these SMAP-derived datasets. A multi-scale analysis of these datasets and SWAMPS (at 25km resolution and downscaled) will assess the trade-offs between spatial resolution, temporal coverage and product fidelity. We are currently developing these inundation retrieval algorithms using simulated SMAP data from Uninhabited Aerial Vehicle Synthetic Aperture Radar (UAVSAR).

2.3. **Mapping delta vulnerability based on changes in water and sediment flux and ocean conditions (CU)**

The spatial pattern of river sediment replenishment of the coastal zone of deltas and delta progradation in general are directly influenced by the magnitude of the flux, as well as the dispersal of fluvial sediments by waves and current when entering the ocean. Magnitudes and timing of fluvial fluxes towards the coast and ocean are commonly controlled by seasonality. In addition, much of the flux may be delivered to the ocean during low frequency, high magnitude events. Persistent differences in wave energy and direction during the high river discharge season, or during short-lived high magnitude freshwater events, influences the dispersal of sediments across the coastal zone. Once sediments are deposited on the shelf, consolidation processes initiate, making it more difficult to resuspend them over time. Consequently, even the landward flux of resuspended sediment by waves and storms may be controlled to some extent by the precise conditions at time of original deposition.

We analyzed model simulations to determine wave conditions during seasons and high magnitude discharge events. The Water Balance Model and sediment flux model (WBMsed, Cohen et al., 2014) is used to quantify timing and magnitude of river water and sediment fluxes, and WAVEWATCH III® is used to determine the ocean regime.

A 50-year, 1960-2010, daily simulation of WBMsed provides terrestrial river sediment fluxes on a 6-arc minute spatial scale to the ocean for the entire world. WBM takes daily rainfall and temperature data (from the NCEP/NCAR reanalysis climatological data), global maps of vegetation, land-use, irrigation and soil properties (Wisser et al., 2010), and then calculates the hydrological balance for each of its gridcells. Runoff is routed through streams and river drainage basins with a Muskingum mass balance solution to determine river discharge. This model has recently been advanced to include an empirical sediment flux model (Syvitski and Milliman, 2007; Cohen et al., 2014).

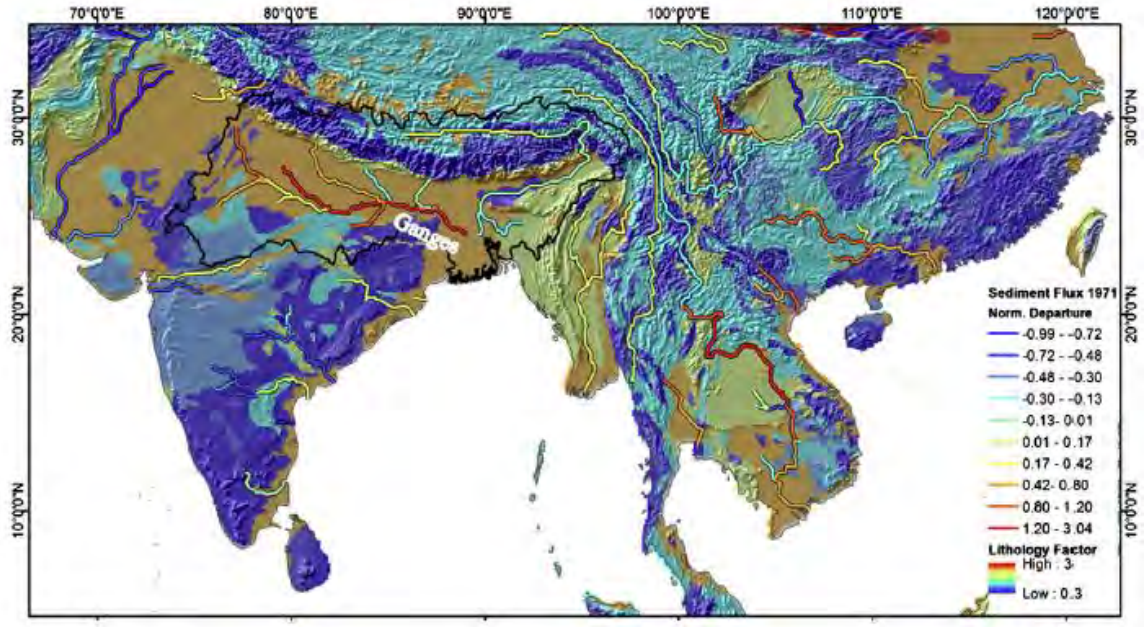

Fig. 7. Sediment flux towards the 5 case study deltas. Figure from Cohen et al. (2014).

Forced by NCEP Climate Forecast System Reanalysis Reforecast (CFSRR) homogeneous data set of hourly 1/2◦ spatial resolution winds, WAVEWATCH III® is used to generate a 30-year, 1979-2009, 1/2◦ spatial resolution wave climatology, made available by the Environmental Modeling Center of NOAA. For our study, 31 deltas of the world were selected, including the 5 selected case study deltas. We identify for each delta for a 30 year period: 1) what are the prevalent ocean conditions at times of delivery of the majority of the river sediment fluxes, and 2) how often do low frequency, high magnitude discharge events coincide with local high wave energy conditions.

Swells, or surface gravity waves are generated by non-local, more persistent weather systems at the ocean and can travel long distances. Swells typically have a long wave period (larger than locally-generated short waves), so although they occur less frequently, they do generate significant wave energy and thus potentially can significantly affect the coastal zone. The Ganges–Brahmaputra delta region is known for its swells, which are typically formed during the monsoonal season (May through September). Swells can inundate low elevation deltaic coastal areas and have the potential to resuspend and disperse sediments in the shallow offshore and even to erode the land-ocean boundary.

To analyze the significance of the energy that a deltaic region receives by swells, the 30-year, 1979-2009 wave climatology of WAVEWATCH III® has been analyzed for swells at a 1◦ spatial resolution, taking into account swell frequency, duration, seasonality and direction. The data generation and processing is completed for 31 deltas, including the 5 selected case studies. A paper of the comprehensive analysis is in progress and will be submitted by early 2016.

2.4. **Continued analysis of susceptible regions: The Ganges-Brahmaputra Delta (CU)**

Fig. 8. Study area of Higgins et al. (2014) in the Ganges-Brahmaputra Delta.

Last year, we reported the submission of a manuscript which included Interferometric Synthetic Aperture Radar (InSAR)-derived subsidence maps over the Ganges-Brahmaputra Delta, Bangladesh (Fig. 8). This manuscript has since been published in the August 2014 volume of Journal of Geophysical Research – Earth Surface (Higgins et al., 2014). The study reconstructed subsidence rates over the period 2007 to 2011 in the eastern portion of the delta, covering more than 10,000 km at a high spatial resolution of 100 m. The study area ranged from the densely populated capital city of Dhaka on the western side of the Indian-Burma Platelet boundary to the city of Raipur on the eastern side of the plate boundary. It crossed both urban and agricultural regions and sampled a wide variety of stratigraphic settings. Global Positioning System (GPS) receivers located in both Dhaka and Raipur allowed calibration and validation of the results (Fig. 9)

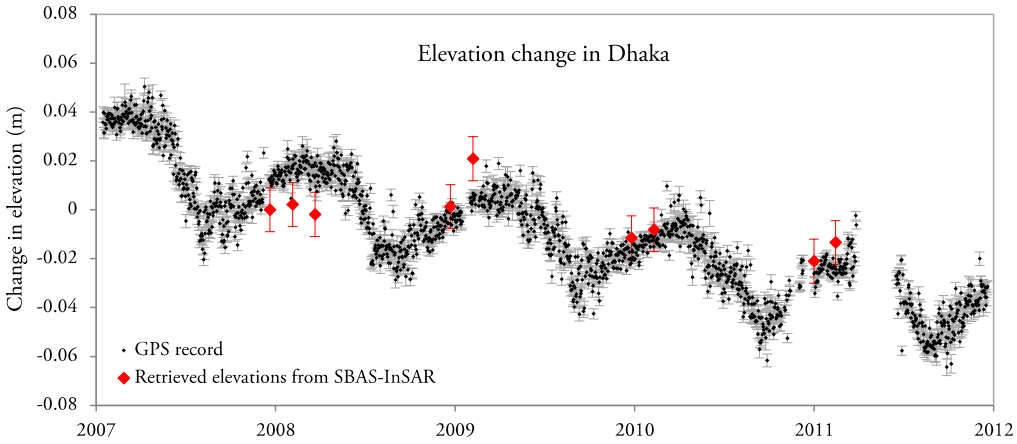

Fig. 9. InSAR-derived elevation change in Dhaka (red) agrees with GPS measurements (black) within uncertainty. From Higgins et al. (2014).

Land subsidence of 0 to > 10 mm/yr was seen in Dhaka, with variability likely related to local variations in shallow subsurface sediment properties. Outside of the city, rates varied from 0 to > 18 mm/yr, with the lowest rates appearing primarily in Pleistocene Madhupur Clay and the highest rates in Holocene organic-rich muds.

In addition to providing a valuable assessment of subsidence rates and variability in the delta, this study demonstrated that subsidence in this delta is primarily controlled by local stratigraphy, with rates varying by more than an order of magnitude depending on lithology. The paper was recently selected as an "AGU Research Spotlight" and was highlighted online and in the 1 Feb 2015 issue of EOS, Transactions of the American Geophysical Union.

2.5. **Methods of employing remote sensing for coastal ocean syndrome detection (CU)**

A manuscript is currently in preparation with the title "On the application of InSAR to sinking deltas." The manuscript is by invitation and will be submitted to Hydrogeology Journal's special issue on land subsidence with a projected publication date of Jan. 2016. The paper discusses the measurement of land subsidence due to fluid extraction in deltas, with a focus on InSAR and its benefits and limitations with respect to measuring such signals in deltas. It also reviews instances of fluid extraction-induced subsidence that have been measured with InSAR in deltas. A discussion of challenges associated with the delta environment follows; these challenges include high humidity, vegetated and/or periodically inundated groundcover, dense forests, rapid growth in megacities that renders Digital Elevation Models (DEMS) inaccurate, and a lack of in situ GPS (Global Positioning System) receivers for InSAR calibration. Processing options are

compared, and recommendations are provided to achieve the highest quality InSAR measurements in a delta setting.

Figure 10, an interferogram over the Ganges-Brahmaputra Delta, shows phase changes from land motion, but it also includes unwanted signals due to soil moisture changes in drying rice paddies and shrimp ponds. Another unwanted phase contribution comes from the difference in interaction between the vegetated areas (Sundarbans Mangrove Forest and tree-lined levees), the L-band radar used to produce the interferograms, and the C-band radar used to produce the Shuttle Radar Topography Mission (SRTM) Digital Elevation Model. Thus, a three-pass processing chain that eliminates the C-band Digital Elevation Model is recommended for delta settings in Higgins et al. (2015) (in prep.)

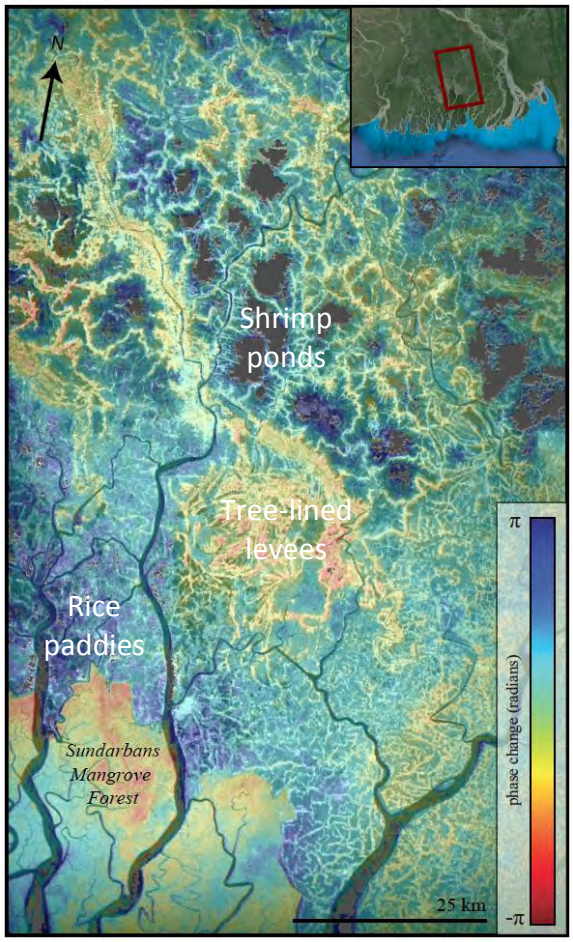

Fig. 10. Interferogram of the Ganges-Brahmaputra delta

2.6. **Synoptic-scale delta risk profiling and future vulnerability scenarios (CUNY)**

Ongoing efforts to construct a delta risk outlook index are nearing completion. We have adapted risk-assessment methods used at local and regional scales to global-scale datasets for ranking and comparison of global deltas-at-risk. Our risk outlook index, an estimate of how risk, or expected loss, is increasing relative to other deltas, is constructed from three sub-indexes: an index of relative sea level rise and wetland loss, which results in increased population exposure to flood events; an index of hazardous event magnitude and frequency; and an index of vulnerability, assessing the relative damage caused by exposure to flooding conditions. Together, these risk components define a risk-space, shown in Figure 11. These results highlight the impact of social vulnerability on risk. Deltas in wealthy nations, particularly the Han, Mississippi, and Rhine, have substantially reduced risk due to investments in risk-reducing technologies such as storm surge barriers and levees, as well as a greater capacity to respond to hazardous events.

The deltas with the greatest expected increases in risk due to relative sea level rise are the Krishna and Ganges. These estimates are in a per-capita sense, when considering risk aggregated across populations, the Ganges is by far the most at-risk, with both the second-highest risk outlook and more than twice the population of the second-most populous delta, the

Nile. We also identify several deltas where their high vulnerability strongly exacerbates already high-risk conditions. A given increase GDP or government effectiveness, resulting in reduced vulnerability, would have the largest effect on risk-reduction in the Limpopo, Irrawaddy, and Krishna deltas.

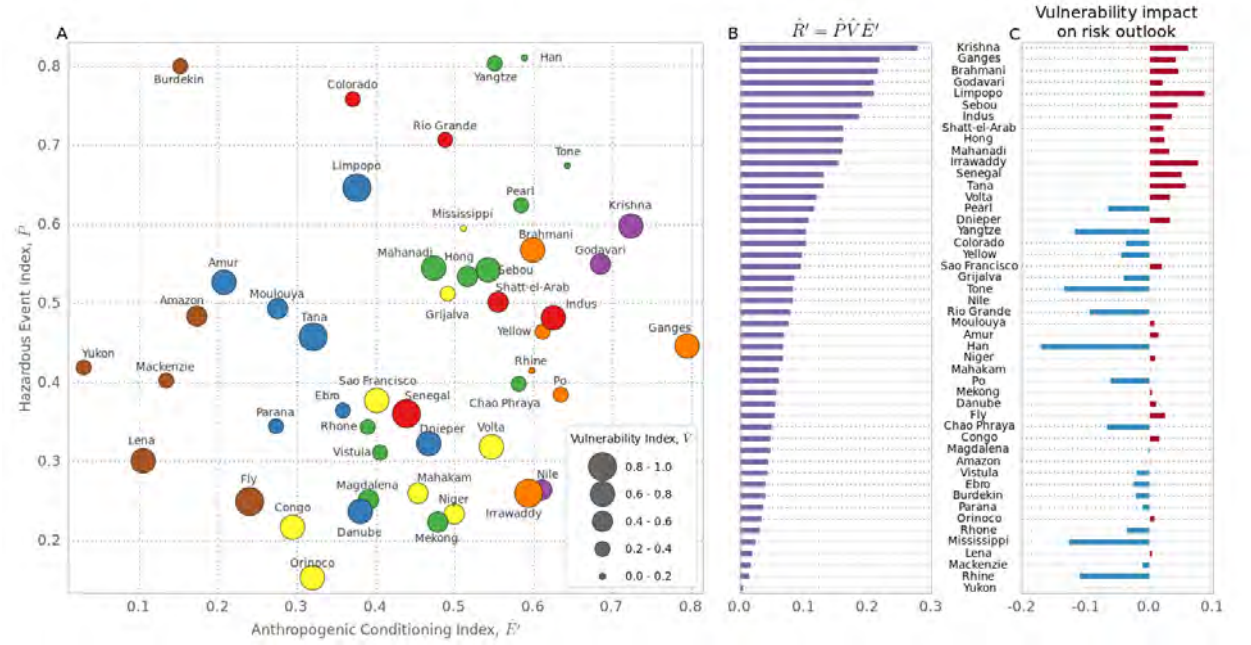

Fig. 11. A) Empirical delta risk space. Color indicates delta cluster, or mode. B) Risk outlook by delta. C) Influence of vulnerablity component on risk outlook.

We also construct a future scenario of large-scale changes in social vulnerability to hazardous events to explore the consequences for delta risk. As seen in Fig. 11C, several developed deltas have substantially reduced risk when contemporary vulnerability is considered, including the Han, Mississippi, Rhine, Tone, and Yanztze deltas. The vulnerability estimate here is an index constructed from total delta GDP, per-capita GDP, and a Government Effectiveness indicator, intended to reflect the amount of harm resulting from flood exposure in a given delta community. The GDP indicators reflect how deltas populations protect themselves: at the delta-scale through engineering projects such as storm-surge barriers, pumping stations, and levees; and at the individual scale through safer housing and protective investments. The government effectiveness indicator expresses the role local and regional governments play in directing GDP toward better hazard preparedness.

However, it has been suggested in the literature that deltas and other environments that depend on external energy and financial inputs are less sustainable than self-reliant systems, particularly in light of potentially higher energy costs in a fossil-fuel constrained future. For comparison with contemporary delta vulnerability, we construct a future vulnerability index by reducing the weight given to the GDP indicators, reflecting higher costs. This adjusts each delta in the risk-

space, with high-GDP/low-vulnerability deltas such as the Mississippi and Rhine experiencing the most change. This identifies delta systems most at-risk for future increases in flood-related expected loss. Figure 12 shows the risk ranking for each delta system under three scenarios: A) Contemporary estimates of risk rank due only to geophysical hazards and anthropogenically-accelerated relative sea level rise; B) Contemporary estimates of risk rank when considering the effect of risk-reduction investments and reduced vulnerability; and C) Future estimate of risk rank with discounted investment effects. While contemporary risk trends are greatest in deltas in Southeast and East Asia (Fig 13A), largest future risk-rank changes are estimated in the Mississippi, Rhine, Han, and Tone (Fig 13B), highlighting the dependence of these high-hazard, high-exposure deltas on their low vulnerability, which may not be the case in the future. This work is being prepared for *Science*, and we expect to submit the manuscript for review shortly.

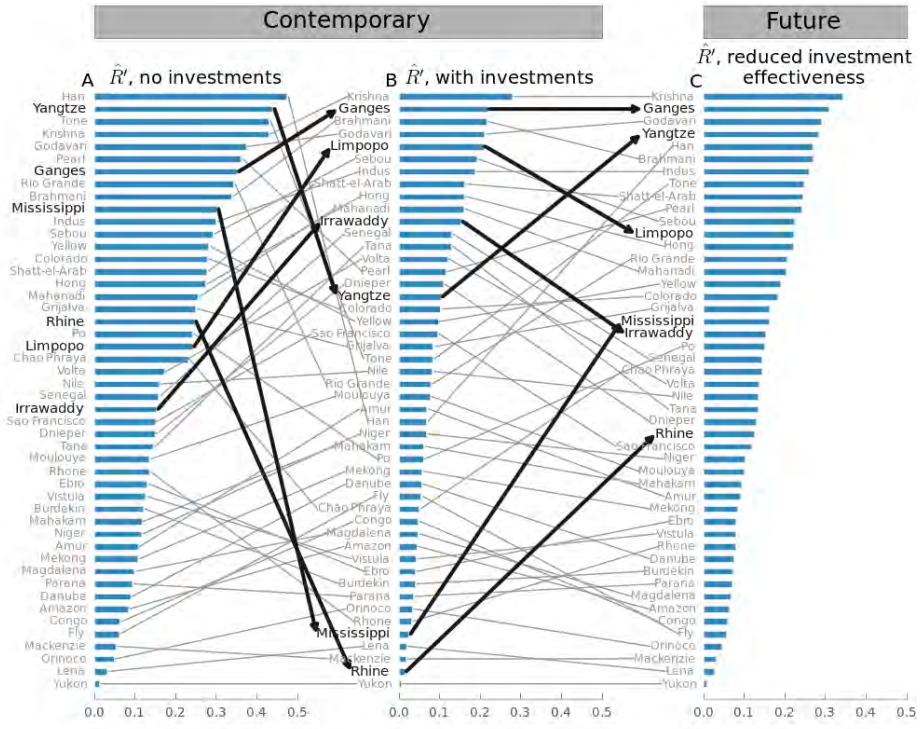

Fig. 12. Contemporary and Future estimates of risk rank changes due to availability of vulnerability-reducing investments. With reduced investment effectiveness, future scenario ranks (C) approach those in (A), particularly for the Mississippi, Rhine, and other wealthy deltas.

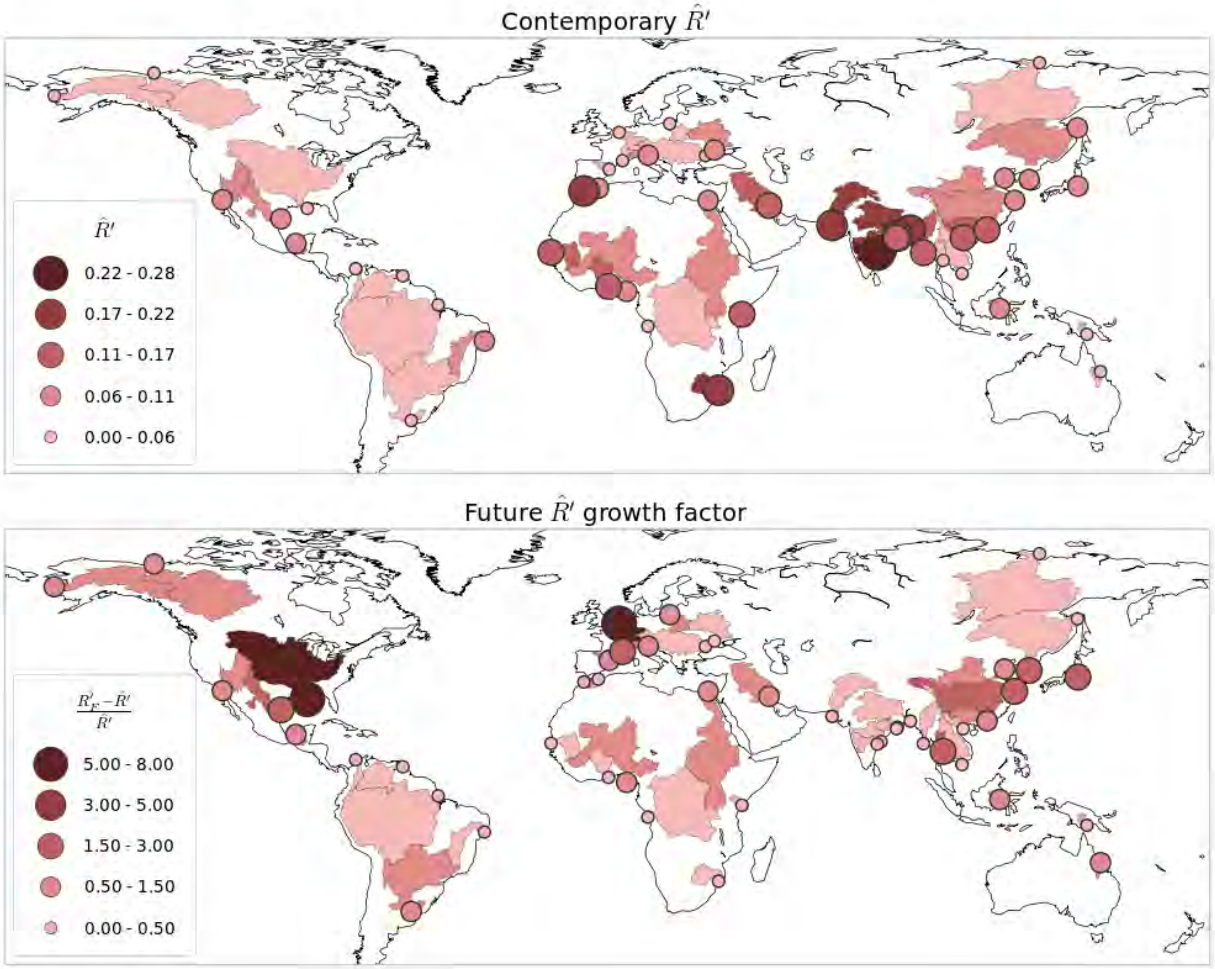

Fig. 13. (A) Current risk trends. High values of $\hat{R}'$ are found globally: the highly populated deltas of Southeast Asia, and deltas in developing parts of Africa and the Middle East. (B) Estimated 50-year growth in future risk trend, $\hat{R}'_F$, relative to current $\hat{R}'$. Highest relative growth in future $\hat{R}'_F$ are in the Rhine, Mississippi, Han, Tone, and Chao Phraya, all systems where current risk is reduced through investments enabled by high GDP and affordable energy costs, relative to the future scenario.

2.7. **Empirical delta inundation modeling in case study deltas (CUNY)**

As an application of the inundation remote sensing work discussed above in Section 2.2, we are investigating the hydrological relationships between observed inundation and modeled river discharge, observed precipitation, and modeled wave energy, and how this varies spatially and temporally. This work is first being done in the Mekong delta, with intentions to expand to other case study delta systems. Previous work investigating surface inundation as a function of local and remote hydrological drivers has relied on inundation models tuned to particular river basins. Utilizing the SWAMPS remotely-sensed inundation product, we are developing spatially-explicit inundation modeling methods applicable across delta systems.

In the Mekong, we have constructed an ordinary least squares linear model mapping river discharge (WBMplus hindcast), local precipitation (TRMM 3B42), and offshore waves (CSIRO Global WAVEWATCH III hindcast) to inundation (SWAMPS). River discharge is currently a single-dimension time-series of input at the delta apex; upcoming improvements to WBMplus should enable river discharge distribution throughout the delta. Precipitation is aggregated to the 25km-pixel size of SWAMPS. Waves, like discharge, is a one-dimensional time-series of average wave energy within 150km of the delta coast. Early results suggest promise in identifying dominant regions of influence for each hydrological driver, after removing the seasonal component of each signal. Figure 14 shows areas of delta with a statistically significant linear relationship between river discharge (left) and waves (right). Discharge is most related to surface inundation in the upper-delta, suggesting the delta river network and agricultural practices in the lower delta decorrelate the river signal from inundation. In contrast, waves are important only within approximately 50km of the coastline.

This work, including a detailed analysis of spatio-temporal subsampling methods to compare higher-resolution precipitation observations with the coarser SWAMPS inundation, is currently being prepared for publication, and was presented at the "*Deltas in Times of Climate Change II*" International Conference in Rotterdam, The Netherlands, in September, 2014.

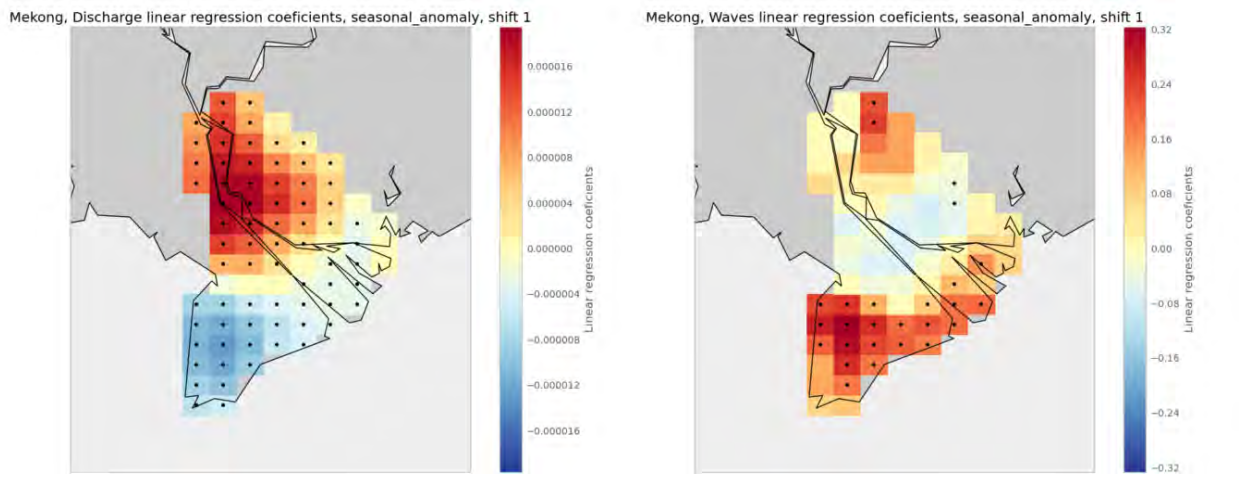

Fig. 14. Linear regression coefficients for river discharge (left) and wave energy (right) regressed on surface inundation, after removing seasonal signals. Discharge appears to be an important driver of inundation only in the upper delta, near the main river stem. Waves are important within about 50km of the coast. Dots indicate statistical significance at the $p<0.05$ significance level.

2.8. **Coastal ocean sediment modeling and sensitivity to delta river network structure (CUNY)**

Building on last year's efforts to develop and test a coastal ocean sediment transport model of the Mekong coastline, we've begun conducting experiments on the model sensitivity to the delta river network water and sediment flux distribution. At the land-ocean interface, river deltas mediate the flux of water, sediment, and nutrients from the basin watershed, through the complex delta river network, and into the coastal ocean. In the Mekong river delta, irrigation networks and surface water storage for rice cultivation redistribute, in space and time, water and sediment fluxes along the coastline. Distribution of fluxes through the delta is important for accurate

assessment of delta land aggregation, coastline migration, and coastal ocean biogeochemistry. Using a basin-scale hydrological model, *WBMsed*, interfaced with a coastal hydrodynamics/wave/sediment model, *COAWST*, we investigate freshwater and sediment plumes and morphological changes to the subaqueous delta front. There is considerable uncertainty regarding how the delta spatially filters water and sediment fluxes as they transit through the river and irrigation network. By adjusting the placement and relative distribution of *WBMsed* discharge along the coast, we estimate the resulting bounds on sediment plume structure, timing, and morphological deposition patterns.

The *COWAST* modeling system is used to develop a coupled hydrodynamics (*ROMS*), waves (*SWAN*), and sediment model of the Mekong Delta coastal zone for the year 2006. A high-resolution, ~1.6 km resolution grid is nested in a coarser, ~8 km resolution regional grid. The nesting has been found to be very helpful for maintaining reasonable background sediment concentrations in the nested grid. The *ROMS* model has 10 vertical levels; the nested grid timestep is 80 seconds, and the coarse grid timestep is 400 seconds. Coupling with *SWAN* occurs every 3 hours. Boundary conditions for *SWAN* are provided by a global *WAVEWATCH III* hindcast simulation. A global 1/12° *HYCOM* simulation provides *ROMS* boundary conditions. Tidal forcing is extracted from the *TPXO7.2* tidal inversion database. *ERA-Interim* renalysis atmospheric conditions are used for ocean surface forcing.

The baseline simulation shows high levels of surface sediment compared with MERIS, though coastal patterns are in good agreement (Fig. 15, 16). The region of very high surface sediment along delta front is well simulated. Seasonality is also captured, with elevated surface sediment in December compared to July. High modeled surface sediment appears to be derived from initial sediment on seabed. Eroded sediment dominates the surface concentration, except very close to river plume. In the simulation with zero initial bed sediment, elevated sediment levels are only seen close to the river mouths. Both simulations appear to capture the relative sediment plume patterns.

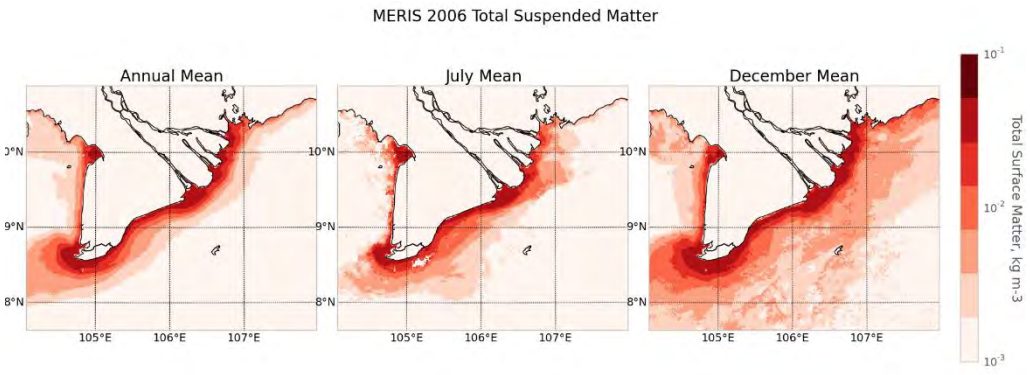

Fig. 15. MERIS 2006 Total Suspended Matter. Compare with simulated results in Fig. 16.

The *COAWST*-based coastal Mekong Delta model is able to simulate the extent and approximate timing of surface sediment plumes, though the background concentration is strongly dependent on initial sediment conditions, suggesting that excess initial bottom sediment is being eroded.

Fluvial fluxes dominant only near the main distributary channels (Fig. 17), where changes to fluvial sediment loads have a strong effect on bathymetric change.

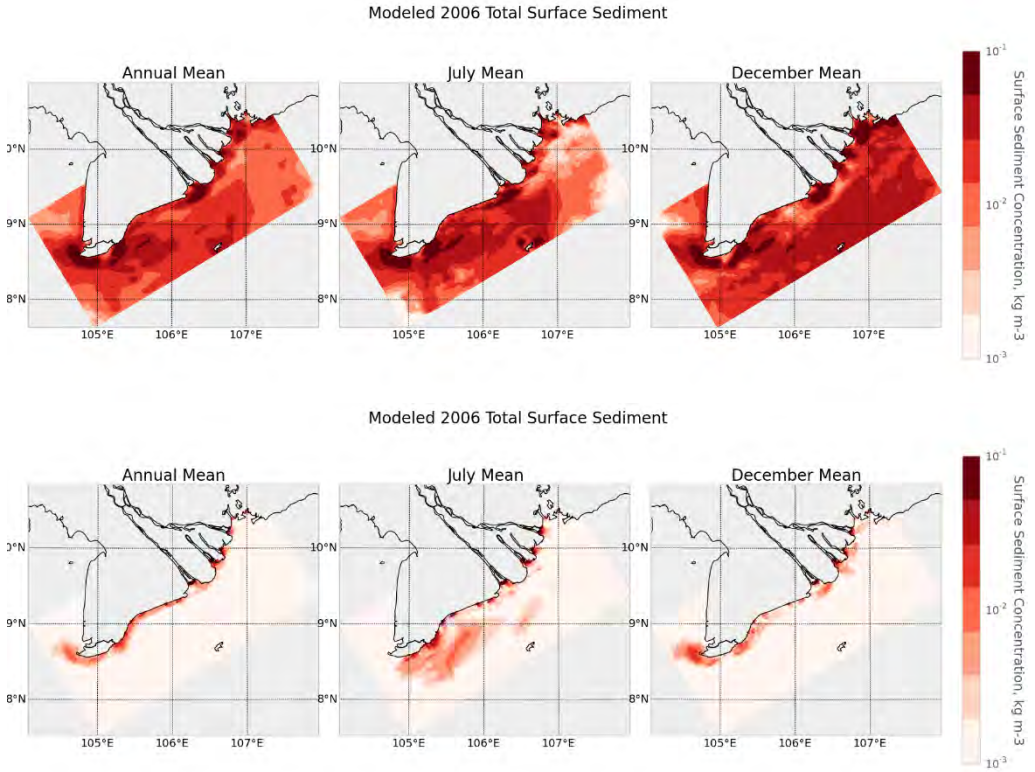

Fig. 16. (Top) Modeled surface sediment with 10m initial bottom sediment. (Bottom) Modeled surface sediment with no initial bottom sediment. Compare with Fig. 15.

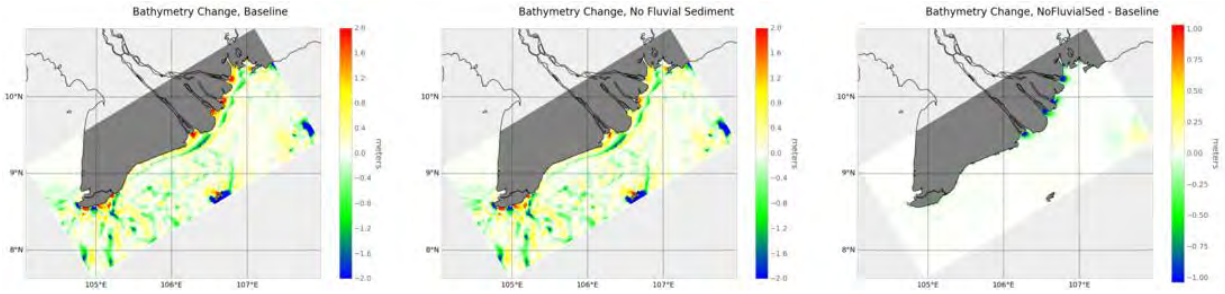

Fig. 17. Two Mekong River sediment distribution model experiments. Left: Bathymetric change after one year, baseline experiment with WBMsed sediment fluxes. Center: Bathymetric change with no fluvial sediment input. Right: Difference between model experiments, highlighting the limited region of influence. Most of the simulated bathymetric change in the domain is due to erosion and deposition of initial sediment on the sea floor.

Ongoing efforts are directed at improving the surface sediment plume expression, as compared with MODIS and MERIS surface observations, with the goal to determine surface plume signatures of human influences on the delta river network.

3. Outreach

3.1. Science on a Sphere

Model output examples are made available to a larger public in collaboration with the NSF funded CSDMS project, by presenting simulations on Science On a Sphere (SOS). SOS, developed by NOAA, is a spherical display system approximately 6 feet in diameter, which can present “movies” of animated Earth system dynamics. We have developed animations, lesson material and running exhibit ‘fact slides’ for two Science-on-a-Sphere (SOS) animations of models, used for this NASA study: a) Global Wave Dynamics (WAVEWATCH III®) (Fig. 18), and b) Global River Runoff, with special focus on (Water Balance Model-WBMsed) (Fig. 19). The development of the early prototypes of the animations and lesson material has been in close cooperation with the education and outreach team of the Fiske Planetarium at the University of Colorado and NOAA SOS technicians. The evaluated lesson material and animations are made available as datasets through the SOS animation library and is available to 33 million people who see Science On a Sphere® every year worldwide. See also: http://sos.noaa.gov/Datasets/

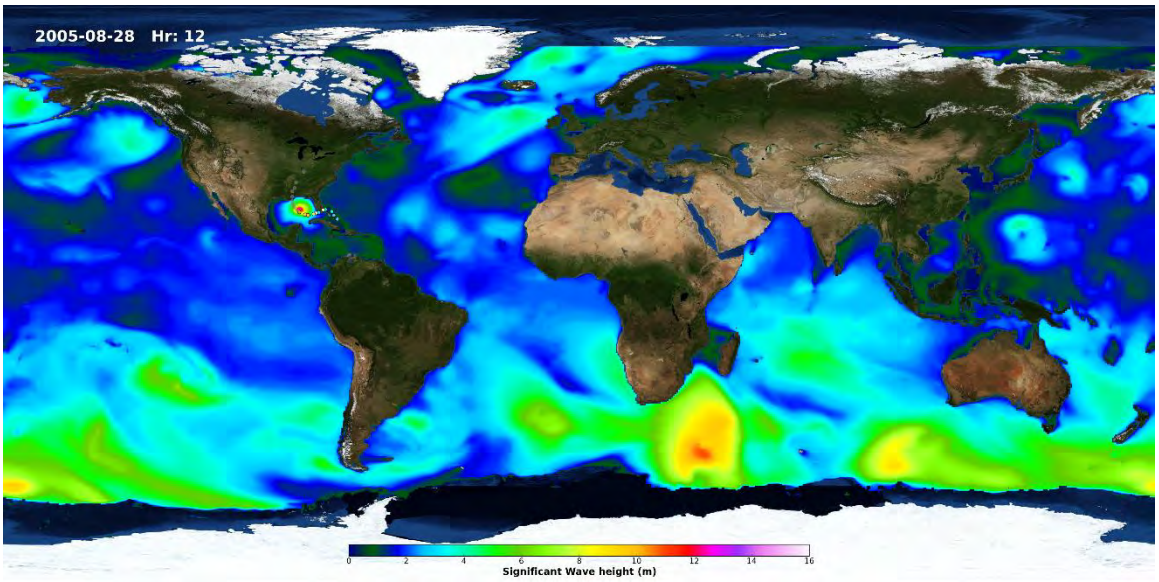

Fig. 18. Significant wave height, simulated with WAVEWATCH III®. For this specific SOS project the storm track of Hurricane Katrina is provided with the Saffir–Simpson hurricane wind scale.

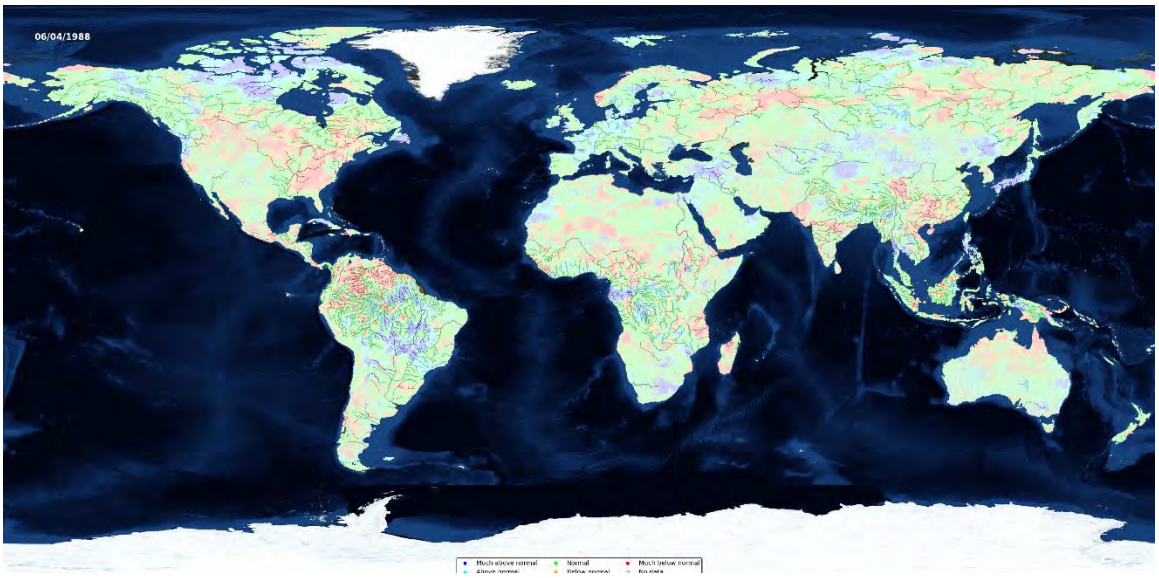

Fig. 19. Representation of WBMsed water discharge simulation, were the colors indicate if the water discharge is above average, normal or below average for any specific day, based on 50 years of simulation data.

3.2. **Undergraduate mentorship through RESESS program**

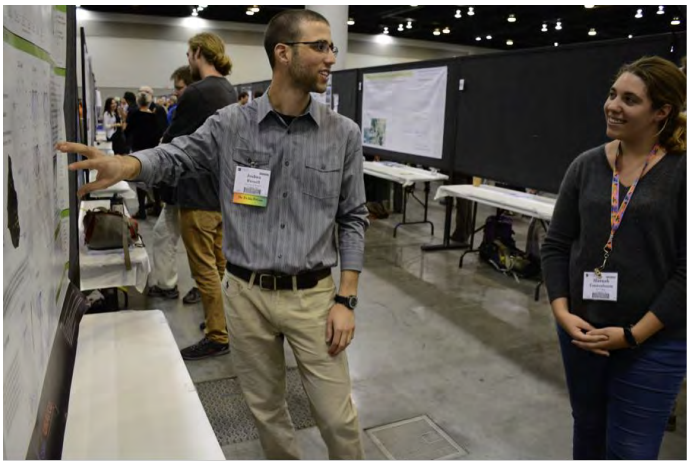

Fig. 20. CU RESESS intern Josh Russell presents at AGU

In summer 2014, University of Colorado Boulder researcher Stephanie Higgins mentored an undergraduate through the Research Experiences in Solid Earth Science for Students (RESESS) Program. RESESS is an NSF-funded undergraduate internship and support program based at UNAVCO in Boulder, Colorado. Each summer, RESESS accepts 10 student interns who are members of a group that is historically underrepresented in the Earth sciences. Josh Russell, the CU group's student, completed an 11-week research project and was mentored in the preparation of a research paper, graduate school and fellowship applications, and a presentation at the annual meeting of the AGU in December 2014 (Fig. 20).

3.3. **Undergraduate data visualization research**

As part of a course taught by Co-I Grossberg, City College of New York undergraduate students Andrew Fitzgerald, Ian McBride, and Ebenezer Reyes developed a web-based data visualization project utilizing surface inundation, precipitation, river discharge, and wave energy datasets in the Mekong and Ganges-Brahmaputra River Deltas. The student website is still in the development stage and not yet publicly available, but a screenshot is of one component of the site is presented in Figure 21. The goal of the site is to provide an interactive exploration of

surface inundation time-series and spatial patterns in the two deltas, highlighting patterns and anomalies.

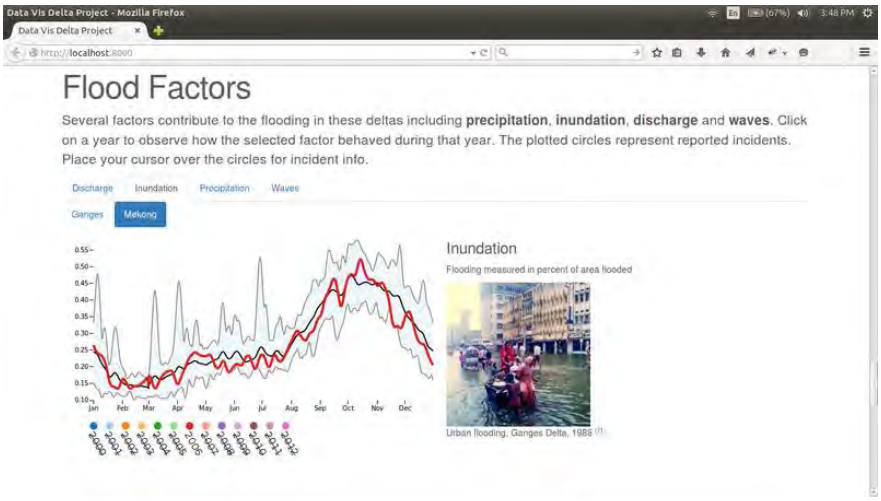

Fig. 21. Example screenshot from student-developed interactive data visualization website.

4. Presentations

- Cohen, S., Kettner, A.J., Syvitski, J.P.M., and Yamazaki, D., *Global-scale simulation of river-floodplain water and sediment exchange within a riverine modeling framework*. AGU, San Francisco, CA, USA, 15-19 Dec. 2014.
- Cohen, S., Kettner, A.J., Syvitski, J.P.M., *Spatially and Temporally Explicit Prediction of Sediment, Nutrients and Water Discharge in Global Rivers*. AAG, Tampa, Florida, USA, 8-12, Apr. 2014.
- Higgins, S., *Measuring land subsidence at the coastal zone*, 39th Annual Natural Hazards Research and Applications Workshop, Broomfield, CO, 22-25 Jun. 2014.
- Higgins, S., Overeem, I., Syvitski, J.P.M., Steckler, M., Seeber, N. A., and Akhter, H., *InSAR measurements of compaction and subsidence in the Ganges-Brahmaputra Delta, Bangladesh*, CSDMS 2014 annual meeting, Uncertainty and Sensitivity in Surface Dynamics Modeling, Boulder Colorado, USA, May 20-22, 2014.
- Higgins, S., Overeem, I., Syvitski, J.P.M., Steckler, M., Seeber, N. A., and Akhter, H., *Monitoring delta subsidence with Interferometric Synthetic Aperture Radar (InSAR)*, GC21D-0574, 2014 Fall Meeting, AGU, San Francisco, Calif., 15-19 Dec. 2014.
- Overeem, I., and Kettner, A.J., *Sedimentation patterns in Fluvio-Deltaic systems.* Nanjing University, Nanjing, China, 14 Oct. 2014.
- Overeem, I., Higgins, S.A., Syvitski, J.P.M., Kettner, A.J., and Brakenridge, G.R., *The Impacts of Armoring our Deltas: mapping and modeling large-scale deltaplain aggradation*. AGU, San Francisco, CA, USA., 15-19 Dec. 2014.

- Tessler Z.D., Vörösmarty C.J., Cohen S., and Tang H. *River network uncertainty and morphodynamics in the Mekong Delta: Model validation and sensitivity to fluvial flux distribution.* AGU Fall Meeting, San Francisco, CA, December 2014.
- Tessler Z.D., Vörösmarty C.J., Foufoula-Georgiou E., and Ebtehaj A.M.. *Spatial and temporal patterns of rainfall and inundation in the Amazon, Ganges, and Mekong Deltas.* Deltas in Times of Climate Change II, Rotterdam, The Netherlands, September 25, 2014.
- Syvitski, J.P.M., *Coastal Subsidence*, 2014 Science Workshop, UNAVCO, Boulder CO, 4-6 Mar. 2014.
- Syvitski, J.P.M., *Rivers of the Anthropocene*, Rivers of the Anthropocene, Indiana University-Purdue University, Indianapolis (IUPUI), 23-25 Jan. 2014.
- Syvitski, J.P.M., *The Peril of Deltas: India and elsewhere - Welcome to the Anthropocene*, IGBP Symposium, Bangalore India, 07 Apr. 2014.
- Syvitski, J.P.M., *The Global Water Cycle in the World of the Anthropocene*, 7th Int'l Scientific Conference on the Global Energy and Water Cycle, The Hague, The Netherlands, 14-18 Jul. 2014.
- Syvitski, J.P.M. & Higgins, S.A., *Subsidence and Relative Sea-level Rise in Threatened Deltas*, H31L-01, 2014 Fall Meeting, AGU, San Francisco, Calif., 15-19 Dec. 2014.
- Vörösmarty, C.J., Tessler, Z., Marchand, M., Phi, H.L., Overeem, I., Kuenzer, C., Renaud, F., Sebesvari, Z. *Science-to-Action: Aligning science with stakeholder and community needs in the Mekong and other delta systems*. Workshop, Deltas in Times of Climate Change II, Rotterdam, The Netherlands, September 26, 2014.
- Xing, F., Kettner, A.J., Syvitski, J.P.M., and Atkinson, J., *Hydrodynamics and morphological changes of the Wax Lake Delta (WLD) during Hurricane Rita, 2005,* CSDMS 2014 annual meeting, Uncertainty and Sensitivity in Surface Dynamics Modeling, Boulder Colorado, USA, May 20-22, 2014.

5. Publications

- Cohen, S., Kettner, A.J., and Syvitski, J.P.M., (2014), Global Suspended Sediment and Water Discharge Dynamics Between 1960-2010: Continental trends and intra-basin sensitivity. *Global and Planetary Change* 115: 44-58. DOI: 10.1016/j.gloplacha.2014.01.011
- Gao, J.H., Jia, J., Kettner, A.J., Xing, F., Wang, Y.P., and Gao, S., *submitted*. The impact of reservoirs on fluvial discharge and sedimentation processes of the Changjiang River, China. Quaternary International.
- Giosan, L., Syvitski, J., Constantinescu, S., and Day, J. (2014), Protect the world's deltas, *Nature* 516: 31-33.
- Higgins, S., Overeem, I., Steckler, M. S., Syvitski, J. P.M., Akhter, S. H., and Seeber, L., (2014), InSAR measurements of compaction and subsidence in the Ganges-Brahmaputra Delta, Bangladesh. *Journal of Geophysical Research – Earth Surface* 119: 1768-1781.
- Sebesvari, Z., Renaud, F., Tessler, Z., Haas, S., Vogt, N., Tejedor, A., Szabo, S., Brondizio, E., Kuenzer, C. Vulnerability indicators for deltaic social-ecological systems: a review. *Abstract accepted by Sustainability Science, in prep.*

- Syvitski, J.P.M., Cohen, S., Kettner, A.J., and Brakenridge, G.R., (2014), How important and Different are Tropical Rivers? – An overview. *Geomorphology* 227: 5-17. DOI: 10.1016/j.geomorph.2014.02.029
- Syvitski, J.P.M., Kettner, A.J., Overeem, I., Giosan, L., Brakenridge, G.R., Hannon, M., and Bilham, R., (2014), Anthropocence metamorphosis of the Indus Delta and lower floodplain. *Anthropocene* 3: 24-35.
- Tessler, Z., Vörösmarty, C.J., Grossberg, M., Gladkova, I., Aizenman, H. A global empirical typology of environmental change in deltas: anthropogenic drivers and implications for sustainable management. *Abstract accepted by Sustainability Science, in prep.*